

# Calibration of gradient propagation delays for accurate two-dimensional RF pulses.

N. P. Davies<sup>1</sup>, P. Jezzard<sup>1</sup>

<sup>1</sup>Centre for Functional Magnetic Resonance Imaging of the Brain, University of Oxford, Oxford, Oxfordshire, United Kingdom

## Introduction

It is well known that concealed time delays often exist between the application of a gradient waveform and the response of the gradient coils. Furthermore, there are often relative offsets in the physical delays that relate to each gradient axis. Although these system delay errors are usually small, they can lead to significant artifacts in some image acquisition methods. Efforts have been made to characterize delays in the gradient system, for example, in echo-planar imaging (EPI) [1] and projection reconstruction [2]. Hidden delays are also of great significance in the case of multi-dimensional selective RF pulses [3], in which the synchronization of gradient and RF waveforms is critical. A broad approach to compensating gradient distortion (including time shifts) is to measure the k-space trajectory produced in the scanner by the specified gradient waveforms, and feed this back into the design of the RF pulse [4]. The concern of this study was to optimize the accuracy of 2D inversion profiles for selective arterial spin labeling (SASL) [5]. It was noted that the sensitivity of the spatial location of selective volumes using 2D RF pulses to the relative timing of the gradient and RF waveforms could be used to accurately calibrate the physical gradient delays of the system using an imaging experiment.

## Methods

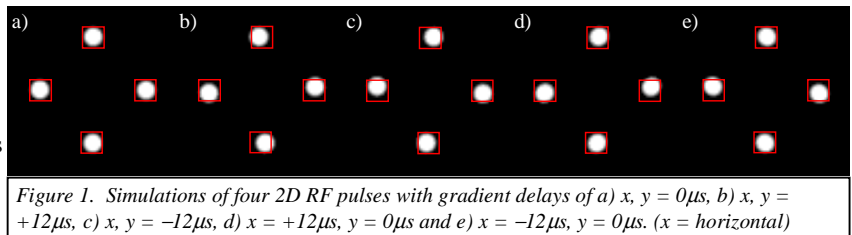
Based on the theory outlined previously [5], RF waveforms were synthesized to produce four Gaussian 2D profiles with a given diameter at equidistant offsets from the iso-centre in the plane of the spiral gradient axes ( $x, y$ ) at  $+x, -x, +y$  and  $-y$ . Bloch equation simulations were carried out to characterize the effects of systematic and axis dependent gradient delays on the spatial profile of spiral 2D RF pulses. Experimentally it is possible to overcompensate for inherent delays, therefore the case of “negative” delays with respect to the RF was also studied. The pulse parameters were: 8000 points, duration ( $T_{\text{pulse}}$ ) 16 ms, 16 spiral turns ( $N$ ), maximum gradient amplitude 18 mT/m, resulting in a pencil diameter of 10 mm. The following equation was derived for the rotation angle  $\theta$  about the isocentre for a time shift  $\Delta t$  of the RF phase relative to the gradient waveforms:

$$\theta = 2\pi \Delta t N / T_{\text{pulse}} \quad (1)$$

A modified SPGR sequence was used to measure the location of the profiles in the scanner, by applying the relevant 2D RF pulse as a saturation pulse prior to excitation. Within the pulse sequence, a delay was introduced between the application of the gradient waveforms and the RF pulse and between the waveforms on each physical gradient axis. These delays were adjusted and the resulting profiles measured. The calibration procedure assumes that any mismatch between the 2D profiles and the target locations is due to uncompensated gradient delays. Given a set of 2D RF profile images with erroneous locations, the propagation delays that could account for the measured discrepancy are then calculated. First, the rotation angle of each profile about the isocentre is estimated by finding the centre of “mass” of the subtraction image. This results in two measurements for each gradient axis, which can be averaged to find the best estimate of the rotation errors. The uncorrected gradient delay on each axis can then be calculated from equation [1]. These values are then used to accurately compensate for the propagation delays in the pulse sequence.

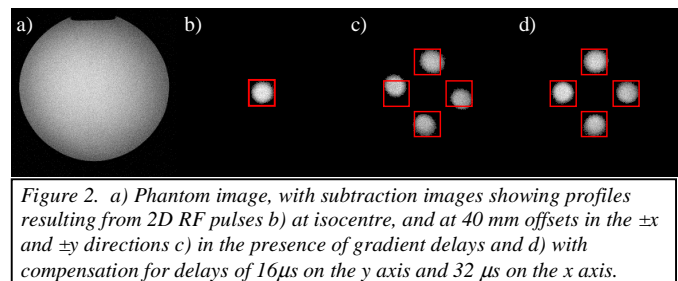
## Results

Figure 1 shows the simulation results, with an image FOV of 80 mm, resolution 1 mm and a 25 mm offset. Fig. 1a illustrates that with the gradient and RF waveforms perfectly aligned, the resultant profiles lie at the predicted locations (indicated by the red box), where the result for each pulse has been superimposed on one image. Fig. 1b-c shows that with a delay on both  $x$  and  $y$  gradients of  $\pm 12 \mu\text{s}$ , each profile rotates about the isocentre by an angle of  $\pm 4.6^\circ$ . Fig. 1d-e demonstrates that if the same delay is applied to the  $x$  gradient independently, a rotation results only in the profiles with an offset in the  $x$  direction.



In general, the simulations showed that for a delay,  $\Delta t$ , in one gradient waveform relative to the RF pulse, the position of a target point with an offset in the corresponding direction rotates by an angle given by equation 1. As expected from the resultant k-space trajectory, with increasing discrepancy between the delay on each gradient axis, there is a distortion in the shape of the profile from circular to elliptical.

Figure 2 demonstrates the gradient propagation delay calibration. Fig. 2b shows a subtraction image of the phantom with a 2D RF saturation pulse applied at isocentre. In Fig. 2c, a series of 2D RF saturation images has been subtracted from the baseline image and then added together. The same 2D RF pulses were used as in the simulations, but the pencil diameter was 16 mm and the radial displacement was 40 mm. From the measured rotations of each profile and using equation 1, a  $16 \mu\text{s}$  delay in the  $y$  gradient and a  $32 \mu\text{s}$  delay in the  $x$  gradient was diagnosed. Fig. 2d confirms that after compensating for these delays, the 2D profiles accurately coincide with the target positions.



## Discussion

This successful calibration procedure works by approximating small concealed gradient delays to a scenario where only the RF phase waveform is shifted relative to the gradients, since changes in k-space sampling and weighting are negligible. The method is sensitive to very small propagation delays, potentially limited only by the gradient waveform resolution. It is likely that some residual eddy current effects may also be compensated by this method, but further characterisation of the interaction between eddy currents and gradient propagation delays is required [6].

## References

- [1] Reeder SB et al. Magn Reson Med 41:87-94 (1999).
- [3] Pauly J et al. J Magn Reson 81:43-56 (1989).
- [5] Davies NP and Jezzard P. Proc ISMRM 10:620 (2002).

- [2] Peters DC et al. Magn Reson Med 50:1-6 (2003).
- [4] Takahashi A, Peters T. Magn Reson Med 34:446-456 (1995).
- [6] Nehrke K et al. Magn Reson Imaging 17:1173-1181 (1999).